Physics – Uspekhi **63** (7) 668 – 682 (2020)

REVIEWS OF TOPICAL PROBLEMS PACS numbers: 64.70.K – , 64.75.Nx

Pairwise interatomic interaction in alloys

Yu I Ustinovshchikov

DOI: https://doi.org/10.3367/UFNe.2019.10.038687

Contents

Abstract. The concepts of the physics of metallic alloys regarding the driving forces of diffusion phase transformations, the nature of solid solutions, the chemical interatomic interaction energy, the principles of plotting phase diagrams, and the principles of heat treatment of alloys are critically reviewed. The ordering–separation phase transition, which is caused by the recently detected property of alloys to change the sign of chemical interatomic interaction when temperature changes, is shown to change these concepts radically. The experimental data that fully support the ideas advanced in this review are presented (comprehensive experimental data for Ni–Cr and Co_3V alloys are presented). The problem of the diffusion processes in multicomponent alloys is considered in detail. They are shown to occur according to the model of pairwise chemical interatomic interaction. The formation of diffusion couples in a multicomponent alloy begins in its liquid state. When temperature decreases, this process occurs in each diffusion couple similarly to the phase formation in the corresponding binary alloys.

Keywords: ordering–separation phase transition, ionic bond ↔ covalent bond electronic transition, diffusion couples

1. Introduction

It was generally accepted that the solid solution in metallic alloys forms when a system of atoms of different elements gives rise to the crystal lattice common to all elements based on the solvent lattice. It was supposed that solubility of any element in the solvent lattice depends largely on the difference between the sizes of solvent and dissolved component atoms. If the difference between the sizes of these dissimilar atoms exceeds 14–15%, the solubility in the solid state is restricted (the 15% rule) and stable intermediate compounds form in the alloy. The theoretical substantiation of this rule was obtained by analyzing the elastic strain energy generated during the formation of solid solutions. It was believed that the difference between the sizes of atoms A and B predetermined the development of elastic stresses inside the crystal lattice of alloys. The magnitude of such elastic stresses determined the degree of solubility of B atoms in the lattice of A atoms and served as the driving force that caused precipitation of 'excess' phases from the solid solution upon a fall in temperature and, therefore, a reduction in solubility. The electron concentration (e/a) was considered to be another important factor influencing both the solubility of the solid state and stability of intermediate phases.

In other words, solid solutions were thought to consist of different chemically noninteracting atoms (ions). The atomic structure of alloys used to be represented graphically in the form of noninteracting adjoining spheres. All known theories of new phase formation regarded a disordered solid solution as the starting equilibrium phase that became 'oversaturated' upon a fall in temperature and therefore gradually decomposed. Chemical interactions between different atoms in solid solutions were considered to manifest themselves only when the atoms of the dissolved component happened to be involved in the formation of 'excess' phase particles. It was deemed that till that instant, chemical interactions between atoms (including dissimilar ones) do not manifest themselves.

Such metaphysical interpretation of the structure of solid solutions and particles was wholly based on the results of experiments carried out long ago with liquid molecular solutions and demonstrating that the solubility of, say, a salt

Yu I Ustinovshchikov Udmurt Federal Research Center,
Ural Branch of the Russian Academy of Sciences,
ul. im. Tat'yany Baramzinoi 34, 426067 Izhevsk, Russian Federation
E-mail: ust@udman.ru

Received 15 May 2019, revised 29 September 2019
Uspekhi Fizicheskikh Nauk **190** (7) 715 – 731 (2020)
Translated by Yu V Morozov; edited by V L Derbov

in water increases with temperature. Although the nature of intermolecular interactions in aqueous solutions is totally different from that of atom-atom interactions in metallic solid solutions, it was supposed that both processes are underlain by the same mechanism, on the assumption of similar precipitation kinetics of excess phase crystals from aqueous solutions and particles of the new phase from solid solutions. In this way such concepts in the theory of alloys, were introduced as solubility of atoms of one component in the lattice of another, direct temperature dependence of solubility, and an oversaturated solid solution borrowed from the theory of aqueous solutions.

The same principles were accepted as a basis for constructing equilibrium phase diagrams, the majority of which depicted solid solution regions at high temperatures and two-phase regions at low temperatures. All these ideas, formulated almost 100 years ago, well before the advent of modern technologies for alloy crystal structure research, such as transmission electron microscopy (TEM), are still used practically unaltered in the physics of metallic alloys.

They were seemingly confirmed in later experimental studies on alloy microstructure with the use of the X-ray diffraction technique. Indeed, this method failed to reveal any other phases except the solid solution in alloys quenched from high temperatures. This suggested that the alloy microstructure at high temperatures had to be a solid solution, in good agreement with the theory of molecular solutions.

There are two points of view as regards the role of rapid water quenching in the formation of the alloy structure. One (classical) is based on the assumption that the values of effective diffusion coefficients of many element pairs well known for different temperatures are such that a well defined length of time (hours or minutes) is needed for diffusion phase transitions to occur accompanied by the dissolution of the former microstructure and the formation of a new one. From this standpoint, quenching in water from a given temperature actually fixes the microstructure (cooling takes fractions of a second) that existed in the alloy at the temperature from which the quenching process was started.

The other point of view became widespread after TEM had come into wide use for the study of alloy microstructures in 1960–1970. At that time, many authors were surprised to discover that the microstructure of the overwhelming majority of alloys quenched from solid solutions in water proved to be two-phase ones either containing particles of the new phase arranged differently in the solid solution or undergoing modulations of the composition [1–6]. Practically nobody doubted that the source of the discordance was the experiment carried out by these authors rather than the phase diagrams taken from reference books. It was speculated that alloy decomposition by the spinodal mechanism occurred during quenching, i.e., for a very short time commensurate with the cooling time in water. Such behavior of the alloys was attributed to the absence of the critical nuclei formation stage in the spinodal decomposition, which allegedly resulted in a sharp acceleration of the nucleation process.

Our earlier publications [7, 8] present a comprehensive explanation of the causes responsible for this situation. The use of X-ray diffraction (XRD) to identify highly dispersed particles of the new phase is strongly limited; they are usually identified by local TEM, which gave rise to a controversy: the XRD data were used to plot phase diagrams, while TEM revealed quite different structures in most alloys inconsistent with those in phase diagrams.

A detailed analysis of these studies has led to the conclusion [8] that solid solution regions in equilibrium phase diagrams are actually two-phase regions, in agreement with the well-known axiom of thermodynamics which asserts that all natural solutions are imperfect and undergo either positive or negative deviations from the Raoult law. Then, the existence of extensive regions of solid solution, which is not an equilibrium phase, in conventional equilibrium phase diagrams is easy to explain bearing in mind that the limited potential of the XRD method which was and is still used to construct phase diagrams fails to identify highly dispersed particles of precipitating phases.

The physics of metals considers the high-temperature state of ordering alloys to be a homogeneous solid solution in which atoms of different components are chaotically distributed over crystal lattice sites and interstices (in substitution and interstitial alloys, respectively). As temperature decreases (when the alloy is believed to become oversaturated with a dopant), it undergoes an order–disorder phase transition. The physical cause behind the ordering is considered (see above) to be the elastic interaction between component atoms that constitute the solid solution [9]. Upon a decrease in temperature, making the interatomic interaction potential much higher than the thermal energy, the mutual arrangement of component atoms in the solid solution is found from the minimum alloy free energy condition [9], leading to the precipitation of a new phase.

2. History of the discovery of the ordering–separation phase transition

An ordering–separation phase transition consists of sign reversal of the energy of chemical interactions between component atoms of an alloy at a certain temperature. This phenomenon was observed in many systems overviewed in [7]. It was conjectured that for each binary system such a transition occurs at a specific temperature, called the ordering–separation phase transition temperature. When the temperature of an alloy goes through the phase transition point during heating or cooling, the sign of the energy of the chemical interaction between component atoms changes as the energy passes through zero. As a result, the microstructure formed within a certain temperature interval near this point is a disordered or almost disordered solid solution. It was thought that the transition temperature is the same for all alloys of a given system but specific to each individual system. Therefore, it was believed that the temperature of this phase transition is possible to determine from the analysis of changes in the microstructure of a single alloy of the system formed after heat treatment at different temperatures (by TEM) or changes in the electron structure caused by heating or cooling of the sample to a certain temperature (by X-ray photoelectron spectroscopy (XPS)).

The discovery of the ordering–separation phase transition, reported for the first time in 1996 [10], made us critically reconsider these views. This transition was shown to occur at a temperature specific to each alloy system that reverses the sign of the chemical interaction between atoms A and B. Earlier authors were of the opinion that each binary system has an inherent ordering energy sign constant at any temperature. Later findings of the ordering–separation phase transition in alloys radically changed this view. They led to the conclusion that the sign of the chemical interaction energy changes as temperature varies, sometimes more than

once. At the beginning, the transition is associated with the alteration of the alloy electron structure as evidenced by a change in the shape of the valence bands in the X-ray electron spectra determined by XPS [11, 12]. A change in the sign of the chemical interaction between dissimilar atoms alters the direction of reciprocal diffusion fluxes between these atoms to the opposite one, which affects the type of microstructure. If an alloy exhibits an ordering tendency (i.e., dissimilar atoms attract one another), chemical compounds form in the structure. Where there is a tendency toward separation, clusters or grains consisting largely of like atoms are formed, while previously existing microstructures disappear.

To find the ordering–separation phase transition line in any binary system, a study of its microstructure and/or electron structure needs to be carried out (by TEM and XPS, respectively) using alloys of at least two different chemical compositions, each located at a distance approximately one third to one quarter of the composition scale. The difference between the chemical interaction energy signs of these two compositions, if any, gives evidence that the ordering–separation phase transition line depends on the alloy concentration too.

The phase diagram in Fig. 1 shows temperatures at which regions showing a tendency toward ordering (σ-phase formation) and those tending toward separation (chromium-enriched particles are formed) exist. No other phase, except the solid solution, can be formed near the ordering–separation phase transition line when the chemical interaction energy is close to zero. In the vicinity of this temperature (which can be either high or low), an alloy has the structure of a disordered solid solution. Farther from the phase transition temperature, the absolute chemical interaction energy may prove too low for the proper new phase to precipitate, which is likely to result in the retention of the solid solution structure. Everything depends on the nature of the alloy, meaning that a band in which the disordered solid solution structure is preserved can exist in the neighborhood of the phase transition line within a certain temperature range.

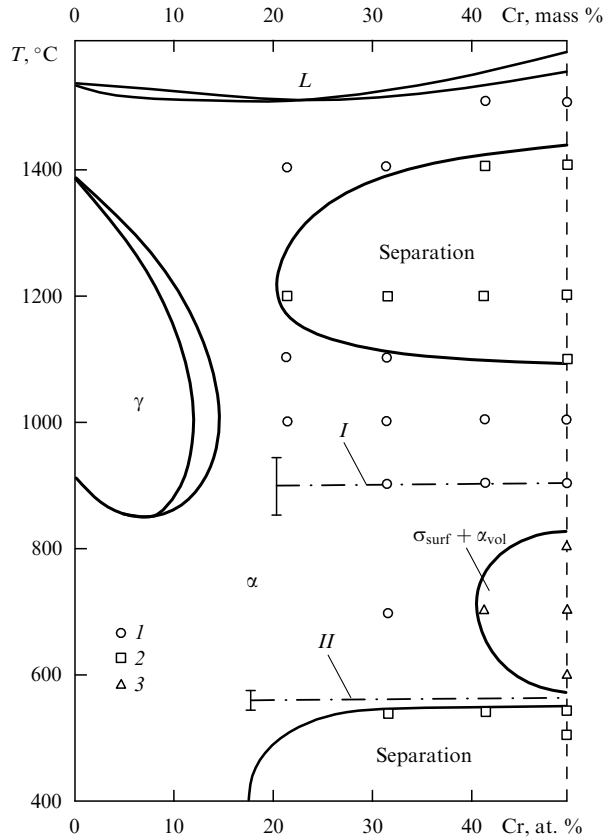

Figure 1. Fe-rich part of the Fe–Cr phase diagram based on results of Ref. [8]. Experimental points: *1* — α-solid solution, *2* — separation structure of high-temperature transition, *3* — separation structure of low-temperature transition. Dash-dotted lines: *I* — high-temperature ordering–separation phase transition, *II* — low-temperature ordering–separation phase transition. Region in the diagram: σ-phase (at the surface) +α-solid solution (in the volume).

The width of the temperature band in which the solid solution structure is observed differs for different systems and temperatures. For example, in an Fe–Cr system where two ordering–separation phase transitions occur, the width of the temperature range within which a disordered solid solution exists during high- and low-temperature transitions is 850 – 1150 °C and 560 – 580 °C, respectively (see Fig. 1) [8]. The absolute chemical interaction energy beyond these intervals is high enough for a chemical compound (the σ-phase) to precipitate in the alloy in the case of a negative sign of the chemical interaction energy of enriched and depleted clusters of component atoms with the positive sign.

3. Energy of chemical interatomic interaction in alloys

It seems appropriate that a discussion of the physical nature of chemical interactions between atoms in alloys should be preceded by the consideration of the issue of terminology usage, including that of such terms as ordering energy, mixing energy, and mixing enthalpy. Each of them denotes, in principle, the same concept but fails to characterize exactly its physical sense. The energy in question in any alloy is due to chemical interaction between the neighboring atoms of which the alloy consists. If the interaction energy has a negative sign, the alloy exhibits an ordering tendency and forms chemical compounds. In the case of a positive sign, the system tends to separate and forms clusters. Therefore, we believe it is reasonable to choose a single term that would most comprehensively describe the physical essence of this energy and call it the chemical interatomic interaction energy in alloys. In the presentation below,we will use exactly this term.

Figure 2 illustrates the temperature dependence of the chemical interaction energy in an $Fe_{50}Cr_{50}$ alloy. The diagram shows the experimentally found ordering–separation phase transition points (*1* and *2*). The points of intersection of the chemical interaction energy curve E and lines *3*, *4*, *5* showing the absolute energy level above which the new phase begins to precipitate were determined from the temperature scale [8] as the points separating the single- and two-phase regions in the Fe–Cr phase diagram (see Fig. 1).

The discovery of ordering–separation phase transitions in alloy experiments gave evidence of a direct dependence of the alloy microstructure on the sign of the chemical interatomic interaction energy E and of the possibility for the solid solution structure formation on the absolute value of this energy. At the same time, the latter two parameters (the sign and the absolute value of E) directly depend on the relationship between the heating temperature of the alloy of interest and the ordering–separation phase transition temperature. It follows from Fig. 2 that two phase transitions (at 560 and 1000 °C) take place in Fe–Cr alloys. The dashed lines *3*, *4*, *5*

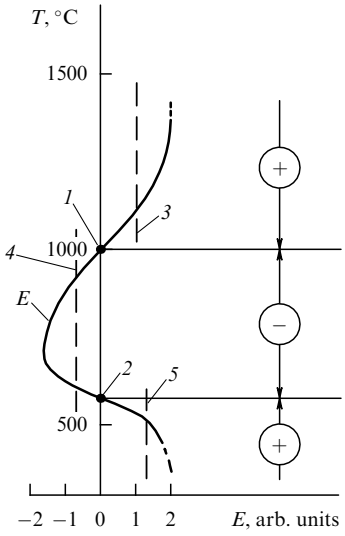

Figure 2. Schematic diagram illustrating temperature dependence of $Fe_{50}Cr_{50}$ alloy chemical interaction [13].

correspond to the level of the chemical interatomic interaction energy (in absolute units) above which the new phase (Cr-enriched clusters or the σ-phase) precipitates in the alloy. The points of intersection of lines *3*, *4*, *5* with the *E* curve correspond to the points in the Fe–Cr phase diagram separating single- and two-phase states of the alloy [8].

The above scheme provides a basis for the following conclusions [8].

1. The chemical interaction between dissimilar atoms is a regular feature of all alloys, regardless of heating temperature.

2. Precipitation of a particular phase and the formation of a solid solution depend on the sign and absolute value of the energy of chemical interactions between dissimilar atoms rather than on the solubility of atoms of one component in the lattice of another.

3. The sign of the energy of chemical interactions between dissimilar atoms is not constant and changes with temperature (sometimes, more than once) in most metallic systems.

4. Each heating temperature corresponds to a definite alloy microstructure that forms after holding at a given temperature; the preceding microstructure is not inherited and disappears.

5. The disordered solid solution structure can form in a temperature region adjacent to ordering–separation phase transition temperatures, i.e., in the phase diagram region where the absolute value of the chemical interaction energy is close to zero.

4. Morphological and kinetic features of the ordering–separation phase transition in binary alloys

By far not in all systems the ordering–separation phase transition leads to such clear division of the phase diagram into regions where ordering, separation, or disordering solid solution microstructures are formed at the phase transition temperature as in alloys of the Fe–Cr system. For example, in the Ni–Co system, the microstructure regions formed due to the ordering and separation tendencies can overlap. This suggests the formation of a region in which microstructures

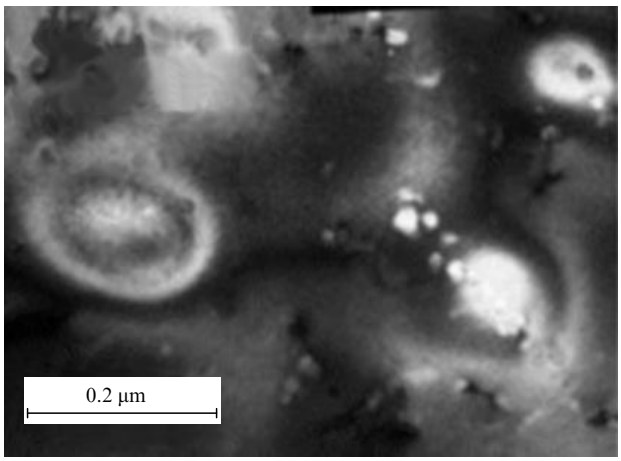

Figure 3. Microstructure of Ni_3Co alloy after aging at 500 °C. The figure shows dissolving clusters of Co atoms (absorption contrast) and particles of the precipitating phase Ni_3Co_2 (diffraction contrast).

showing a tendency toward both ordering and phase separation co-exist near the ordering–separation phase transition temperature instead of the disordered solid solution region (Fig. 3) [13].

This means that the process of transformation of a microstructure formed due to the tendency toward separation into a microstructure resulting from the ordering tendency proceeds somewhat differently than as described earlier [8]. In other words, the process goes through simultaneous dissolution of Co-enriched separation clusters into a composition corresponding to the alloy composition with the formation at other points of the alloy of particles of a chemical compound containing more cobalt than its mean concentration in the (Ni_3Co) alloy [13] rather than through complete dissolution of the separation microstructure and the formation of a disordered solid solution. Results of electron microscopic experiments allow determining the temperature range in which the ordering energy changes its sign: this transition temperature interval lies somewhat above 600 °C.

5. Phase transitions in a cobalt–vanadium system

It is believed that alloys of the Co–V system liberate at 1071 °C and below particles of Co_3V, a chemical compound having an ordered $AuCu_3$-like hexagonal structure with 26 atoms per cell, $a = 0.5032$ nm and $c = 1.227$ nm [14].

A structural study of the Co–18.2% V alloy exposed to a temperature of 800 °C for 168 and 553 h was undertaken in [15]. The authors concluded that in both cases the crystalline structure of precipitates had the form of Co_3V ($L1_2$), but in the former case bright satellite spots appeared near fundamental reflexes and the image showed oval particles, while satellites were weak in the latter case and traces in the image that looked like antiphase boundaries could be observed [15].

Reference [16] reports a study of the Co_3V alloy structure at different temperatures, results of which lead to somewhat different conclusions. The quenching of this alloy was performed from the liquid state. A bright-field image of the structure and an electron diffraction pattern of the alloy (see the inset) are presented in Fig. 4 showing precipitates of an arbitrary shape irregularly arranged in the matrix. The electron diffraction pattern exhibits satellites arising from

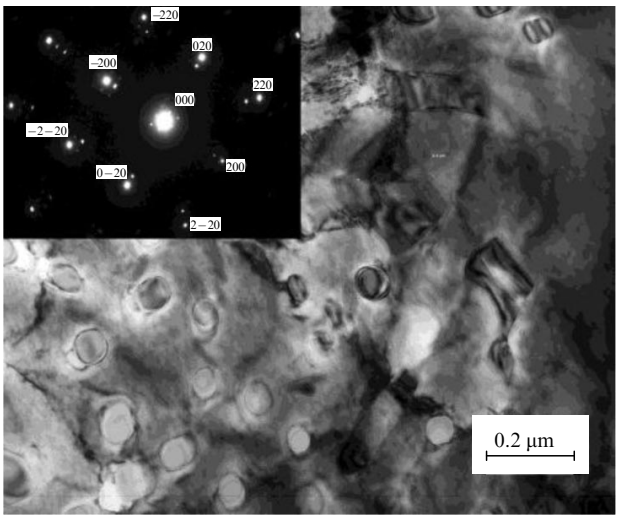

Figure 4. Bright-field image of the structure and microelectron diffraction pattern (inset) of the Co_3V alloy quenched from the liquid state. Particles of V atoms can be seen.

these particles with the BCC vanadium lattice near the main reflexes corresponding to the FCC lattice (see the inset in Fig. 4). This means that particles of the more refractory element, vanadium (having the BCC lattice), undergo crystallization even in a liquid solution due to the separation tendency of the alloy at high temperatures.

A decrease in quenching temperature from 1500 to 1150 °C causes a rise in the absolute value of the chemical interatomic interaction energy as evidenced by a larger size or the number of V particles formed at 1150 °C in comparison with 1500 °C. Figure 5 depicts one such particle after quenching of the alloy from 1150 °C. It is almost an order of magnitude larger than particles in Fig. 4. In other parts of the foil, these particles of virtually the same size as in Fig. 4 aggregate into colonies (Fig. 6). An electron diffraction pattern of such colonies analogous to the one in Fig. 4 (see the inset) also exhibits BCC vanadium satellites. Such enlargement of V atom particles (see Fig. 5) or the formation of large colonies (see Fig. 6) consisting of such particles (Fig. 6) suggests that the absolute energy of chemical interaction between Co and V atoms increases as temperature decreases from 1500 to 1150 °C.

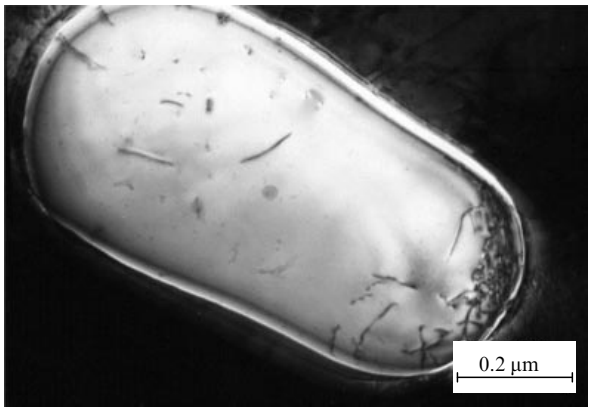

Figure 5. Co_3V alloy. Quenching from 1150 °C in water. A large particle of V atoms.

As the heat treatment temperature falls to 800 °C, two types of structures are formed at different parts of the foil by virtue of separation and ordering tendencies. Such a picture is characteristic of Ni–Co system alloys after thermal treatment at temperatures that cause the ordering–separation phase transition.

For example, Fig. 7, depicting part of a Co_3V foil, shows a structure consisting of very small grains. The authors of [18] argue that this structure is actually a mixture of V-enriched and depleted clusters formed at the temperature corresponding to the onset of separation structure dissolution. The electron diffraction pattern of this structure shows diffuse scattering instead of satellites (Fig. 8). It appears to take place when BCC vanadium atom particles start to dissolve in the FCC Co lattice, i.e., when the ordering–separation phase transition begins.

Other parts of the same foil are home to regions with the newly formed ordering structure as exemplified by the electron diffraction pattern in Fig. 9 showing a system of additional reflexes that suggest $L1_2$ phase precipitation. In light of these reflexes, the dark-field image does not exhibit particles of the new phase; stacking faults alone can be seen. The intensity of additional reflexes in Fig. 9 appears to be too low to allow observation of particles of a chemical compound in a dark-field image. We showed in an earlier study of Fe–Cr [17], Ni–Al [18] and Fe–Ni [19] alloys that the presence

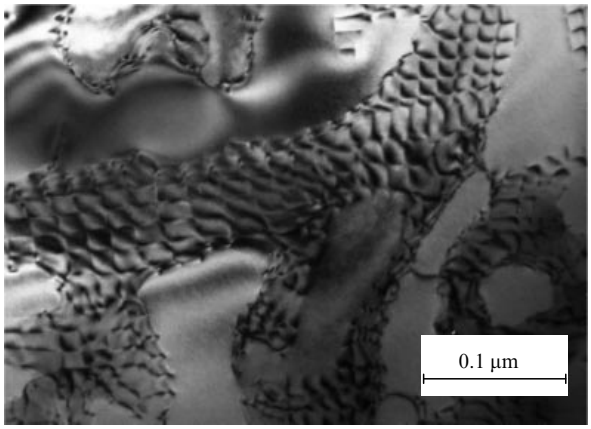

Figure 6. Co_3V alloy. Quenching from 1150 °C in water. Colonies of V atom particles.

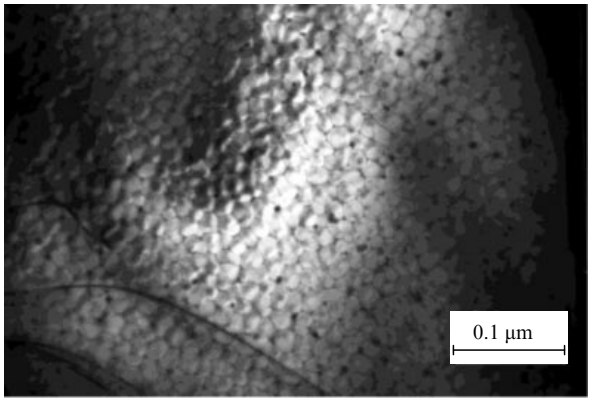

Figure 7. Co_3V alloy. Quenching from 800 °C. Phase separation structure. Bright-field image.

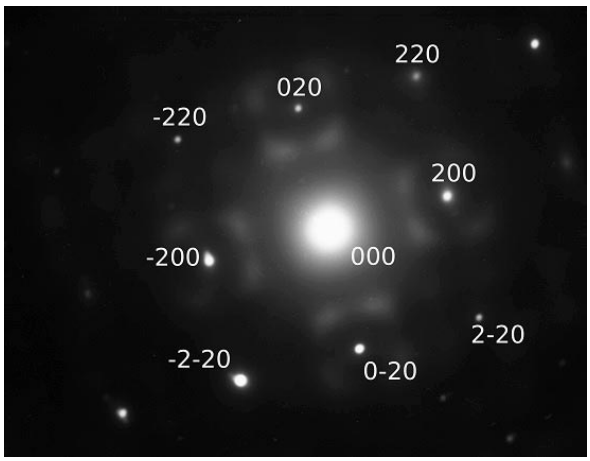

Figure 8. Co_3V alloy. Quenching from 800 °C. Electron diffraction pattern obtained from the structure shown in Fig. 7.

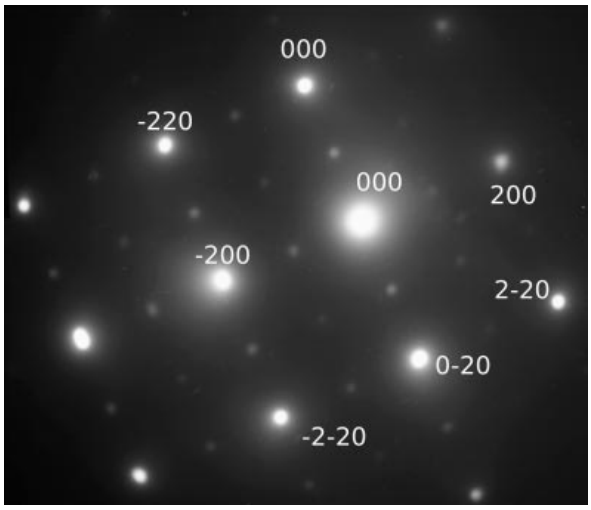

Figure 9. Co_3V alloy. Quenching from 800 °C. Another part of the foil. Electron diffraction pattern suggesting $L1_2$ phase formation.

of a system of new phase reflexes in the electron diffraction pattern and the absence of diffraction contrast from precipitates in the dark-field image possibly suggest that precipitates producing such reflexes are completely coherent with the matrix and do not cause distortion of the lattice at the participate–matrix interface.

The fact that different parts of the foil exhibit different types of microstructures formed during ordering–separation phase transitions suggests that the transition process in the Co_3V alloy does not proceed simultaneously in its entire volume; rather, the quenching fixes the moment when BCC vanadium particles still undergo dissolution in some parts of the foil, while completely coherent particles of the Co_3V compound with the $L1_2$ structure have already precipitated in other parts. The presence of foil regions in which structure formation was due to separation and ordering tendencies in Figs 7–9 enabled the authors of [16] to conclude that a temperature of 800 °C is close to the ordering–separation phase transition temperature. It was mentioned in a preceding paragraph that ordering and separation regions in many other systems are clearly demarcated. Therefore, quenching from the transition region where the ordering energy is close

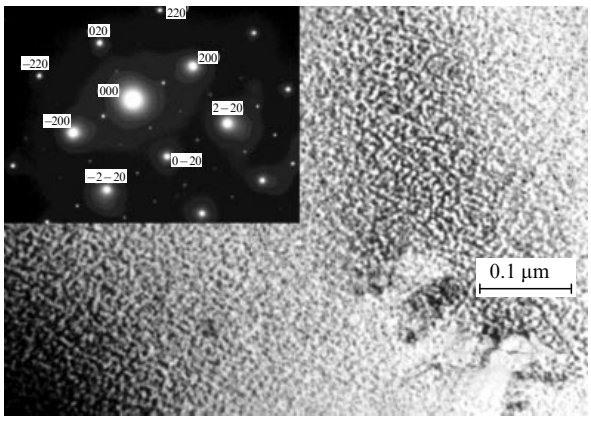

Figure 10. Co_3V alloy. Aging at 500 °C. Bright-field image and electron diffraction pattern (inset).

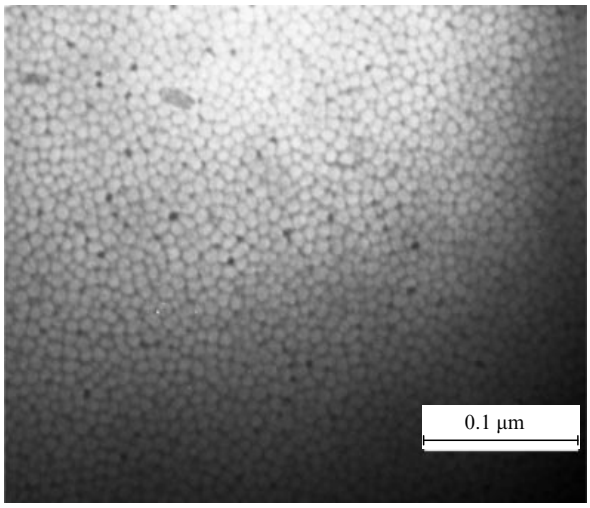

Figure 11. Co_3V alloy. Aging at 350 °C for 10 h. Cellular structure.

to zero may lead to the formation of a disordered solid solution structure.

A further decrease in the heat treatment temperature to 550 °C makes reflexes from the $L1_2$ phase more intense and easier to see (inset in Fig. 10). Moreover, the bright-field image in Fig. 10 allows phase $L1_2$ particles to be observed, suggesting a loss of coherency between the matrix and the particles as the particle size increases.

The aging of an alloy at 350 °C for 10 h makes it possible to observe the separation structure. The authors of [16] hypothesized that this may indicate the existence of one more ordering–separation phase transition in a temperature range from 400 to 450 °C. Figure 11 shows a cellular structure formed after such aging. The cells are smaller than grains after thermal treatment at 800 °C (Fig. 7). Diffuse scattering shown in Fig. 8 is observed again in the electron diffraction pattern. In other words, there are two ordering–separation phase transitions in the Co_3V alloy, at 800 °C and 400 − 450 °C, respectively.

A comparison of these experimental findings with the known phase diagram [14] and plotting the data of the Co_3V study onto the diagram allowed for the conclusion in [16] that the alloy microstructure does not correspond to the data shown in the phase diagram, regardless of temperature. All the results reported in Ref. [16] are reproduced in italics on the

phase diagram [14] in the form of the same kind of abbreviations as those used by the authors of the Co–V diagram [14]. A similar discrepancy between diagrams and the results of electron-microscopic studies of the alloy structure has been described by many researchers [1–6, 10–12], meaning that phase diagrams should be constructed taking into consideration ordering–separation phase transitions in alloys; the lines of such transitions should be plotted onto the diagrams.

6. Specific features of the ordering–separation phase transition in an Ni–Cr system

A diversity of manifestations of the ordering–separation phase transition in different alloy systems can be evaluated from the behavior of an Ni–Cr system. Its chromium-dominated alloys show a tendency toward ordering at any temperature, while Ni-enriched alloys tend to separation, regardless of temperature. Thus far, a single such system is known, and this system is Ni–Cr [20, 21]. In accordance with the universally accepted Ni–Cr phase diagram [14], a eutectic forms in the Ni–Cr system with a composition close to that of the $Ni_{40}Cr_{60}$ alloy, which could mean that alloys of such composition tend to phase separation. However, only one structure showing the ordering tendency was found in the experiment within the entire temperature range examined for this alloy, from the liquid state to 550 °C. For example, Figs 12 and 13 present example bright-field images and the electron diffraction pattern of a sample quenched from the liquid and from 1200 °C, suggesting that irregularly arranged large elongated grains have a Pt_2Mo-type orthorhombic lattice inherent in the chemical compound Ni_2Cr [22, 23]. The formation of Ni_2Cr in a liquid solution means that the $Ni_{40}Cr_{60}$ alloy shows a marked tendency toward ordering even at 1450 °C. In other words, solidification of this alloy begins from the precipitation of Ni_2Cr grains with the Pt_2Mo-type orthorhombic lattice from the liquid solution rather than from the formation of a eutectic consisting of Ni and Cr grains, as is suggested by the diagram.

A decrease in temperature gives rise to fragmentation of Ni_2Cr grains. For example, they are much smaller and arranged more chaotically after thermal treatment at 1000 °C than after quenching at 1200 °C. Treatment at 800 °C causes an even more pronounced fragmentation of the grains and a decrease in their size. Prolonged aging at 550 °C results in a highly dispersed structure in which particles of the chemical compound Ni_2Cr are located at the crystallographic planes of the matrix [20].

Quenching the $Ni_{68}Cr_{32}$ alloy from the liquid state (1450 °C) leads to the formation of the structure shown in Fig. 14. The image displays dark round spots with diffuse edges, considered in Ref. [20] to be clusters of Cr atoms in the lattice of Ni. It appears that the $Ni_{68}Cr_{32}$ alloy is characterized at elevated temperatures by a high energy of chemical interaction between Ni and Cr atoms with the opposite (positive) sign. An analogous structure of the clusters of Cr atoms can be seen in electron microscopic images after quenching the alloy from 1200 and 1000 °C. However, the number of clusters decreased with decreasing treatment temperature, and their contours become even more eroded [21]. The Ni_2Cr phase was altogether absent in this alloy regardless of temperature, even if it was observed earlier (in accordance with the phase diagram) [14] in alloys of a similar composition at temperatures below 590 °C.

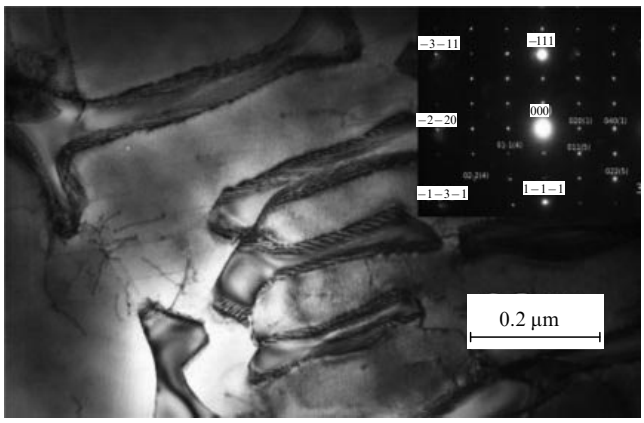

Figure 12. $Ni_{40}Cr_{60}$ alloy. Quenching from the liquid state. Bright-field image of Ni_2Cr phase particles. Inset: electron diffraction pattern obtained from Ni_2Cr phase.

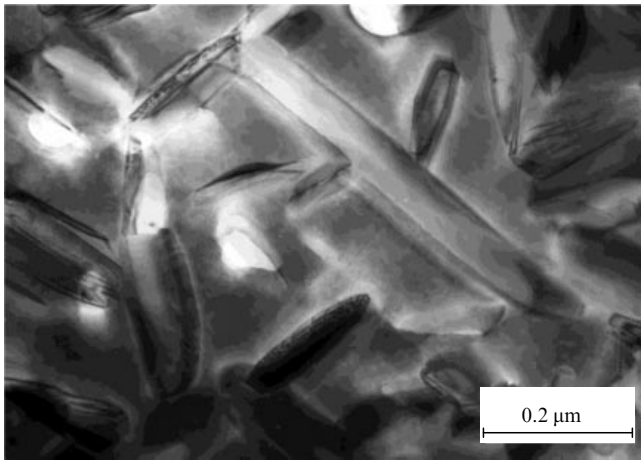

Figure 13. $Ni_{40}Cr_{60}$ alloy. Quenching from 1200 °C. Bright-field image of the Ni_2Cr phase.

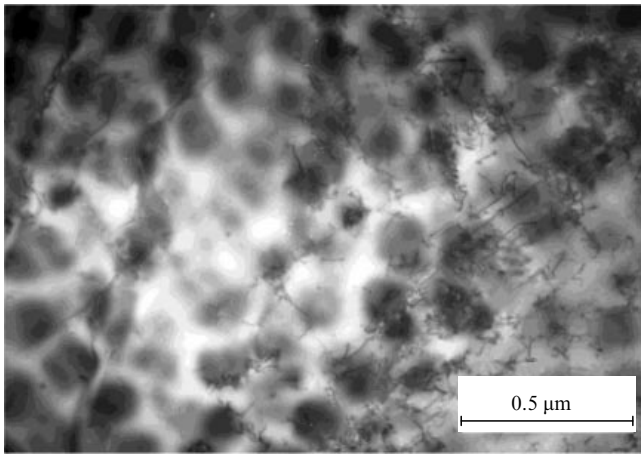

Figure 14. $Ni_{68}Cr_{32}$ alloy. Quenching from the liquid state. Bright-field image of Cr atom clusters (absorption contrast).

The authors of [20] obtained experimental data suggesting that the signs of the chemical interaction between component atoms in $Ni_{40}Cr_{60}$ and $Ni_{68}Cr_{32}$ alloys remain unaltered over the entire heating temperature range; the sign is negative in

the case of $Ni_{40}Cr_{60}$ treatment and positive for $Ni_{68}Cr_{32}$. This means that the boundary between the regions of ordering and separation in the Ni–Cr phase diagram must show a stronger dependence on the change in the alloy concentration than on variations in its heat treatment temperature. Therefore, the objective of the next experiment [21] was to determine the position of this boundary in the temperature-composition coordinates. $Ni_{46}Cr_{54}$ (No. 3), $Ni_{56}Cr_{44}$ (No. 4), and $Ni_{62}Cr_{38}$ (No. 5), whose compositions are within the interval of previously studied $Ni_{40}Cr_{60}$ (No. 2) and $Ni_{68}Cr_{32}$ (No. 1) alloys.

The $Ni_{56}Cr_{44}$ (No. 4) alloy quenched from the liquid state includes high dislocation density solid solution regions intermixed with regions in which clusters of chromium atoms can be observed due to absorption contrast (Fig. 15). Such a combination of regions gives reason to think that the quenching-fixed separation microstructure starts to dissolve in certain regions of this alloy at temperatures above the liquidus line. A decrease in the heat treatment temperature to 1000 °C reveals the ordering microstructure. Figure 16 shows arbitrarily-shaped particles; the microelectron diffraction pattern of a single particle suggests that it has the structure of the chemical compound Ni_2Cr (see the inset in Fig. 16).

The $Ni_{62}Cr_{38}$ (No. 5) alloy was also quenched from the liquid state. Figure 17 is a bright-field image showing absorption contrast from Cr atom clusters spread over the entire foil area. Such clusters form in the liquid state and give evidence that alloys in this state tend to separation. The structure of the same alloy quenched from a lower temperature (1000 °C) contains arbitrarily-shaped particles analogous to those presented in Fig. 16. The aging of the No. 5 alloy at 550 °C resulted in the appearance of dark absorption contrast from oval clusters of Cr atoms against a light background (solid solution). The edges of these clusters are strongly eroded (Fig. 18).

Figure 19 is the commonly accepted Ni–Cr phase diagram with plotted experimental data for No. 1–5 alloys obtained in [20, 21]. The dashed line separating points at which structures showing a tendency toward separation and ordering formed can be regarded as the ordering–separation phase transition line. Its position in the diagram shows a stronger dependence on the alloy concentration than on the heat treatment temperature. The cause of this situation, in which the sign of the chemical interatomic interaction energy depends on both the alloy composition and the temperature of its thermal treatment, remains to be elucidated.

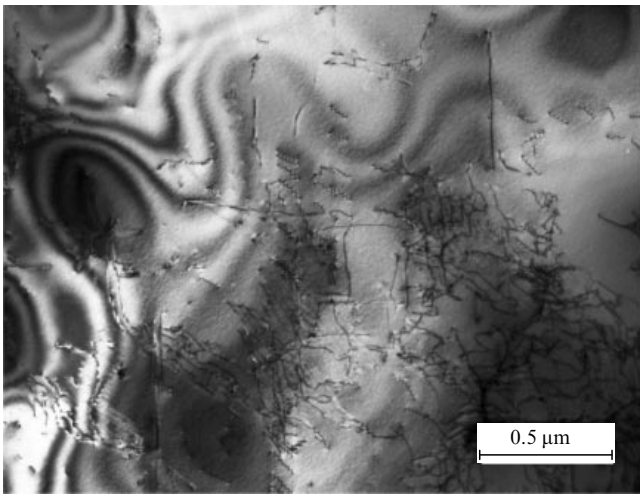

Figure 15. $Ni_{56}Cr_{44}$ alloy. Quenching from the liquid state. Bright-field image.

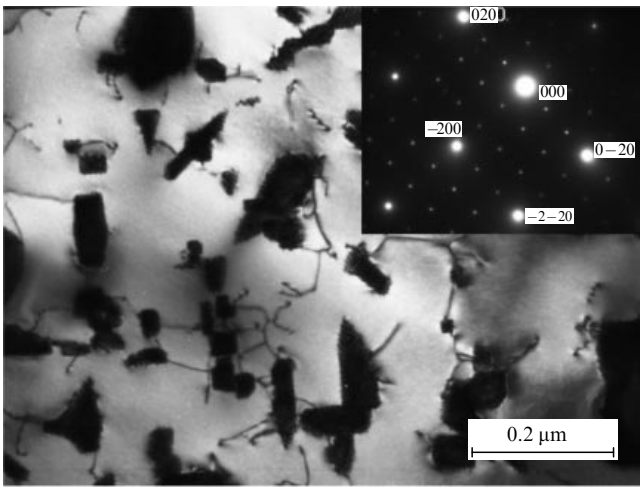

Figure 16. $Ni_{56}Cr_{44}$ alloy. Quenching from 1000 °C. Ni_2Cr phase.

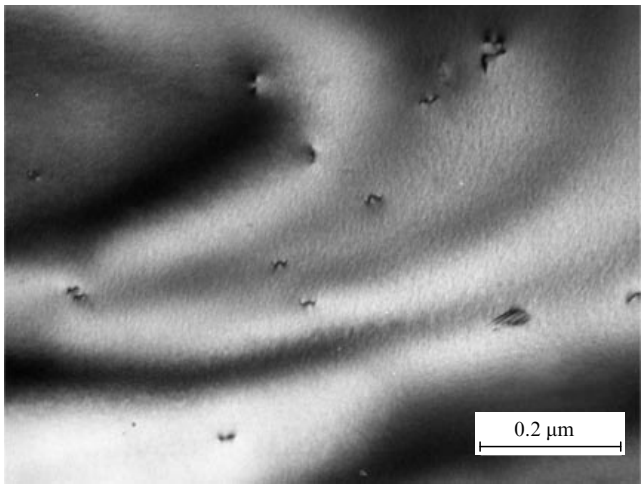

Figure 17. $Ni_{62}Cr_{38}$ alloy. Quenching from the liquid state. Clusters of Cr atoms (absorption contrast).

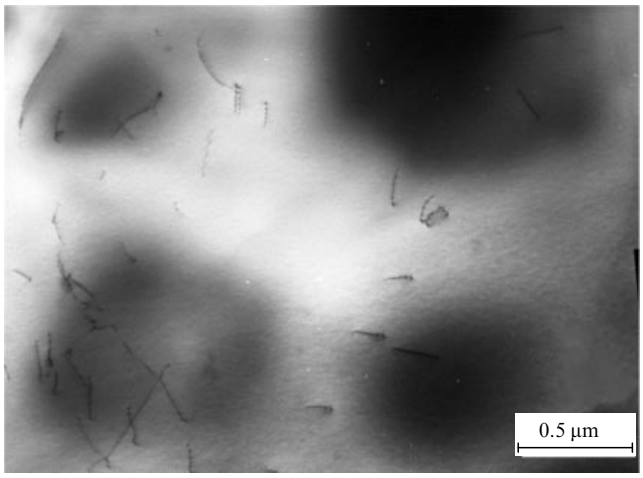

Figure 18. $Ni_{62}Cr_{38}$ alloy. Aging at 550 °C. Clusters of Cr atoms.

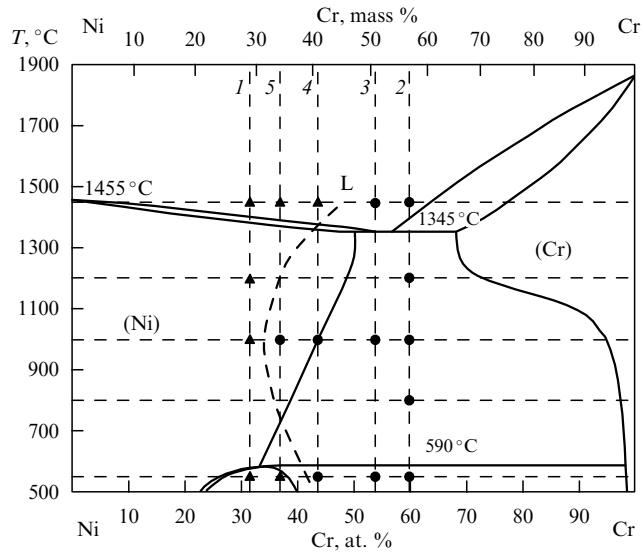

Figure 19. Determination of the ordering–separation phase transition line in the N–Cr diagram. Notations: ● — ordering microstructure, ▲ — separation microstructure.

7. Multicomponent alloys

7.1 $Ni_{50}Co_{25}Mo_{25}$ model alloy

The composition of the $Ni_{50}Co_{25}Mo_{25}$ alloy is chosen so that the number of solvent atoms is equal to the sum of equal numbers of atoms of dissolved components [22]. The diagram in Fig. 20 illustrates the signs of chemical interaction and phase transition temperatures for the $Ni_{50}Co_{25}Mo_{25}$ alloy.

Its quenching from the liquid state results in the appearance of dark round precipitates composed of particles of Mo atoms on one part of the foil (see the micro electron diffraction pattern in the inset of Fig. 21). Another part of the same foil (Fig. 22) shows bright spots 0.1–0.2 μm in size with diffuse edges visible owing to absorption contrast from clusters with a high concentration of Co atoms in the Ni–Co diffusion couple. The conclusion that these are actually cobalt atoms is based on the fact that the exact same bright spot structure is observed in the binary alloy Ni_3Co after its high-temperature treatment (inset in Fig. 22) [22]. Evidently, such clusters are formed without appreciable changes in the parameters of the clusters and the matrix that could cause diffraction contrast. Experimental evidence that the distribution of Co atoms in the Ni–Co diffusion couple gradually changes from a maximum (when only a bright diffusion spot layer is apparent) to 25% Co (when only the layer of isolated stacking fault can be seen) is presented in Fig. 23 [22].

Such alternation of microregions with different chemical compositions enabled the authors of [22] to conclude that they can be regarded as corresponding to Ni/Mo and Ni/Co diffusion couples in terms of chemical composition. The size of these microregions appears to be at least one order of magnitude larger than that of the clusters or particles depicted in Fig. 23. There are no boundaries between the microregions visible in an electron microscope, because the boundary between the diffusion couples, e.g., Ni/Mo (containing particles of Mo atoms) and Ni/Co (where clusters of Co atoms are present) is formed by a homogeneous Ni/(Mo, Co) solution of gradually changing composition.

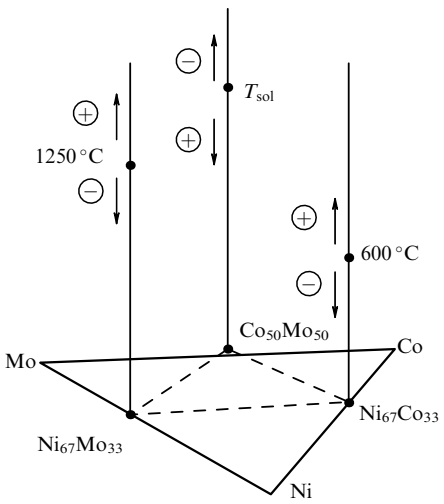

Figure 20. $Ni_{50}Co_{25}Mo_{25}$ alloy. Schematic illustrating interatomic chemical interaction energy signs and ordering–separation phase transition temperature in each diffusion couple.

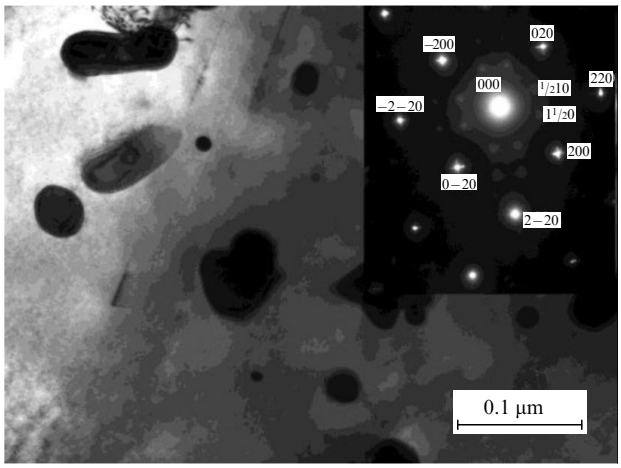

Figure 21. $Ni_{50}Co_{25}Mo_{25}$ alloy. Quenching from the liquid state. Microscopic foil region with particles of Mo atoms. Inset: electron diffraction pattern.

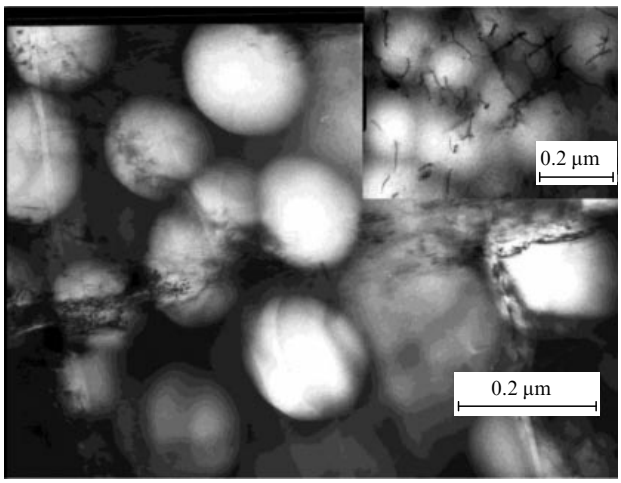

Figure 22. $Ni_{50}Co_{25}Mo_{25}$ alloy. Quenching from the liquid state. Clusters of Co atoms. Inset: clusters of Co atoms in Ni_3Co alloy.

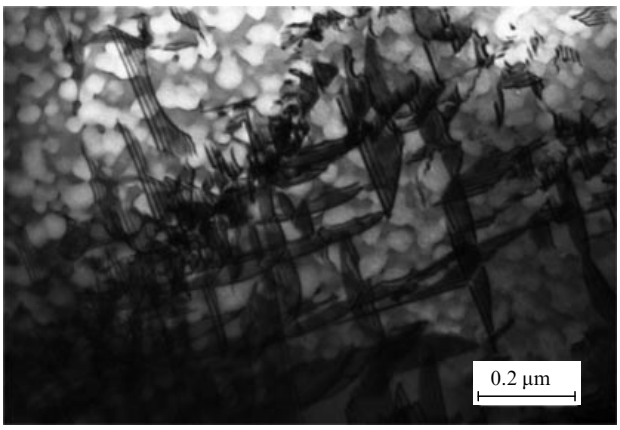

Figure 23. Ni_3Co alloy. Quenching from the liquid state. The third microregion of the same foil. Two layers with different Co content.

Such Co distribution (see Fig. 23) suggests that structures of two types (isolated stacking faults and Co atom clusters in the form of round bright spots) can exist in the matrix as alternating foil layers of varying thicknesses thin enough to enable an electron beam to produce a combined image of these two layers. It can be concluded that Co concentration in an Ni/Co diffusion couple varies over the foil thickness and corresponds to the sinusoidal distribution. This situation can be accounted for only by a tendency toward separation shown by Ni/Co couples in binary Ni–Co alloys at temperatures above 600 °C (see [13]).

Figure 24 illustrates the relationship between the current view of microregions corresponding to one diffusion couple or another and the electron microscopic picture obtained in Ref. [22] using the model $Ni_{50}Co_{25}Mo_{25}$ alloy quenched from the liquid state.

The results reported in Ref. [22] provide a basis for the conclusion that a multicomponent alloy in the liquid state undergoes separation into microscopic sites, the composition of which corresponds to that of one specific diffusion couple of component atoms or another. The same chemical interactions manifest themselves inside these microregions (i.e., inside the diffusion couples) as those taking place in binary alloys of a similar composition at equal temperatures.

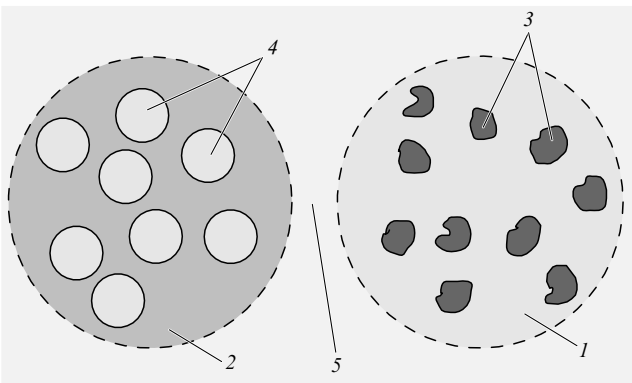

Figure 24. Image of hypothetical microregions *1* and *2* containing two different diffusion couples. Precipitates *3* and *4* in these microregions are morphologically similar to Co atom clusters in the Ni/Co diffusion couple and BCC particles of Mo atoms in the Ni/Mo diffusion couple ($Ni_{50}Co_{25}Mo_{25}$ alloy). *5* — boundary between the two diffusion couples.

A further decrease in temperature leading to a change in the chemical interaction energy sign in a given diffusion couple, i.e., to the ordering–separation phase transition, is accompanied by a change in the type of microstructure in this diffusion couple, while the size of the microregions remains unaltered. This can be accounted for by the significant difference in the diffusion mobility of atoms at liquid state temperatures when diffusion couples are formed and the temperatures of heat treatment of solid state alloys. In other words, the size of microregions containing diffusion couples of a multicomponent alloy formed at temperatures above its melting point remains unaltered by subsequent heat treatment at temperatures below the melting point. It becomes clear why electron microscopy reveals markedly different microstructures at different points of the foil of a multicomponent alloy: it is separated, both in the liquid state and after solidification, into microscopic sites having a chemical composition corresponding to one diffusion couple or another.

7.2 $Ni_{65}Mo_{20}Cr_{15}$ alloy

$Ni_{65}Mo_{20}Cr_{15}$ represents the group of highly corrosion-resistant Ni-based alloys containing molybdenum and chromium. Such materials are known under the general name Hastelloy alloys. Their major advantage is the efficient work when in contact with aggressive media at high pressure and temperature. All properties of these alloys are fairly well known, but microstructural aspects of their formation await further exploration. It is believed that, in a temperature range of 600 – 700 °C, Hastelloy alloys contain particles of the ordered phase $L1_2$ (γ'-phase) responsible for their strength and that the chemical composition of this phase corresponds to the Ni_3(Mo, Cr) ratio [23]. Other authors (see, e.g., [24]) maintain that the strengthening effect on these alloys is associated with the precipitation of the type Pt_2Mo ordered Ni_2(Mo, Cr) phase with a mean particle size of 10 nm.

Diffusion processes in $Ni_{65}Mo_{20}Cr_{15}$ alloys were regarded in Ref. [23] as proceeding in three diffusion pairs: Ni/Mo, Ni/Cr, and Cr/Mo. It was supposed that the process of microstructure formation in these diffusion couples was analogous to that in the corresponding binary alloys of Ni–Mo [12], Ni–Cr [20, 21], and Cr–Mo systems. After quenching the alloy from the solid state (1600 °C), the microstructure in the foil regions containing Ni/Mo diffusion couples was similar to that in the $Ni_{50}Co_{25}Mo_{25}$ alloy

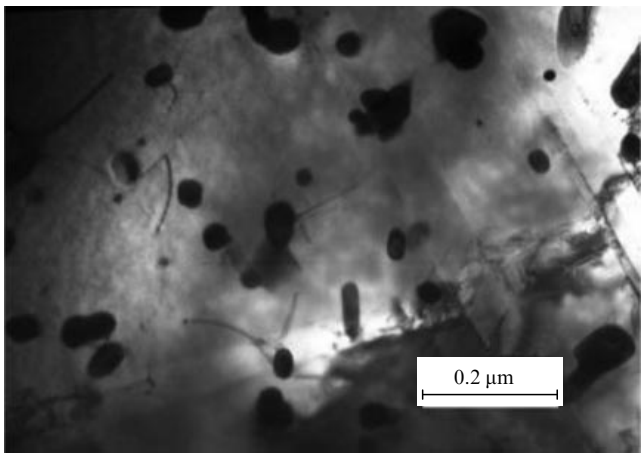

Figure 25. $Ni_{65}Mo_{20}Cr_{15}$ alloy. Quenching from 1300 °C. Particles of Mo atoms.

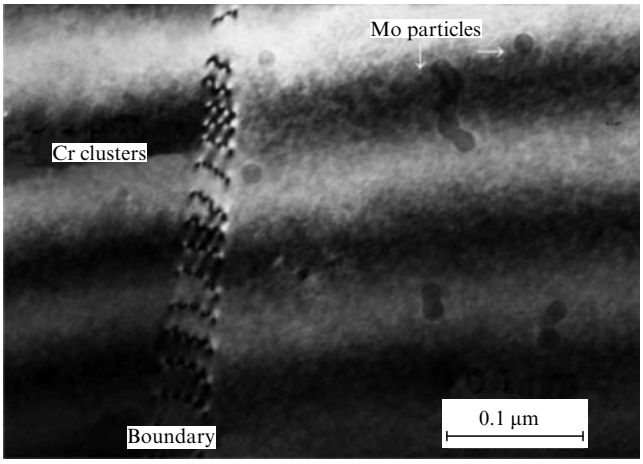

Figure 26. $Ni_{65}Mo_{20}Cr_{15}$ alloy. Quenching from 1300 °C. Clusters of Cr atoms (absorption contrast). Dissolving Mo particles.

(Fig. 25), because the same Ni/Mo diffusion couple formed in both alloys. Particles of Mo atoms were retained in the structure after holding the alloys at 1300 °C for 1 h (Fig. 26). However, their size decreased and no Mo particles were observed at 1200 °C or below, making it possible to determine the ordering–separation phase transition temperature in the Ni/Mo diffusion couple as equal to 1250 °C [23]. This temperature was found to be 1200 °C in a study of Ni–20 at.% Mo and Ni–25 at.% Mo binary alloys by XPS [12]. The results appear to be in reasonably good agreement.

To characterize chemical interactions between atoms in a Cr/Mo diffusion couple, the author of Ref. [23] used data that provided the basis for plotting a commonly accepted phase diagram representing a continuous sequence of solid solutions at temperatures above 890 °C and a phase separation region below this temperature [14]. However, thermodynamic studies of this system at high temperatures showed that the tendency of Cr–Mo alloys toward phase separation is fairly well apparent, even at temperatures much higher than 890 °C. For example, the measurement of partial vapor pressure over the sample surface in the liquid state of this system (1600 °C) revealed positive deviations from Raoult's law [25], justifying the conclusion that alloys of the Cr–Mo system tend toward phase separation regardless of temperature. This suggests that Mo and Cr atoms in Cr/Mo couples can not participate in the co-formation of type Pt_2Mo chemical compound $Ni_2(Mo,Cr)$ or the $L1_2$ type (γ'-phase) compound $Ni_3(Mo,Cr)$. Indeed, the authors of [26] failed to electrolytically extract $Ni_2(Mo,Cr)$ particles from the solid solution of the Hastelloy alloy C-22HS to determine their chemical composition, since the amount of chromium in the precipitate proved much smaller than expected.

Other parts of the same foil (see Fig. 26) displayed periodic absorption contrast waves that can be regarded as resulting from concentration inhomogeneities in the Cr atom distribution inside Ni–Cr diffusion couples of the solid solution. Evidently, such clusters form as a consequence of separation tendency inherent in Ni/Cr diffusion couples at high temperatures [23]. Worthy of note is the marked similarity of cluster shape and position in Ni–Cr diffusion couples of ternary and binary $Ni_{68}Cr_{32}$ alloys.

The concentration of components in Ni/Cr diffusion couples of the alloy corresponds to the part of the Ni–Cr phase diagram dominated by Ni atoms where a tendency toward separation at all heating temperatures and after quenching from the liquid state manifests itself [20, 21]. This means that the Ni/Cr couples in this alloy show the same separation tendency regardless of temperature.

According to the reference literature, the optimal combination of corrosion resistance and viscosity in most Hastelloy alloys is observed after heat treatment at 1150 – 1175 °C (precipitation in the air or water). Results of structural studies indicate that particles of Mo atoms formed at these temperatures when the alloy was in the liquid state are completely dissolved in the solid solution, which leads to the conclusion that the high corrosion resistance of Hastelloy alloys provided by their thermal treatment at 1150 – 1175 °C is due to the following two factors: (1) dissolution of the separation microstructure formed in the liquid state in Ni/Mo diffusion couples in the form of individual particles of Mo atoms; (2) the existence of the separation structure formed in Ni/Cr diffusion couples in the form of clusters having diffuse boundaries with the matrix (see Fig. 26).

7.3 $Co_{53}Mo_{35}Cr_{12}$ alloy

The $Co_{53}Mo_{35}Cr_{12}$ alloy belongs to the group of wear-resistant alloys believed to acquire high strength and hardness due to the formation of coarsely dispersed Laves phase intermetallic particles. Its composition is close to that of well-known Tribaloy alloys based on Co — T-400C or T-800 — and containing approximately the same amounts of Mo and Cr, plus around 2.5% Si and 0.1–0.2%C [27]. Alloys of such composition are usually regarded as hypereutectic, containing 30–70% of the hard intermetallic component distributed in a relatively soft solid solution. The solid primary phase is actually a ternary Laves phase with a melting point of approximately 1560 °C and a composition corresponding to that of Co_3Mo_2Si or CoMoSi. The allotropic nature of cobalt accounts for the precipitation of fcc and/or hcp crystalline structures, depending on the thermal treatment [27]. Primary Laves phase dendrites have a hexagonal structure [28]. The authors of [28] argue that the microstructure of the Tribaloy alloy T-800 contains the Laves phase Co_3Mo_2Si formed during cooling of the alloy after smelting. It is believed that chromium, of all constituent components of the alloy, enhances its corrosion resistance and strengthens the solid solution by raising the probability of a high-temperature fcc $\rightarrow$ hcp phase transition at room temperature [29]. Molybdenum and silicone involved in the Laves phase formation are used to improve the durability of the alloy. Moreover, molybdenum strengthens the solid solution, while cobalt tends to enhance matrix viscosity [29]. For all that, none of the articles cited above provides information on the temperature/time conditions for Laves phase formation and decomposition in Tribaloy alloys.

It follows from the commonly accepted Co–Cr and Cr–Mo phase diagrams with approximately the same ratio of constituent components as in the respective diffusion couples of the $Co_{53}Mo_{35}Cr_{12}$ alloy that only a repelling interaction between Co and Cr, Mo and Cr atoms, i.e., separation, takes place over the entire range of heating temperatures [14]. The tendency toward separation persists in the $Co_{70}Mo_{30}$ alloy within the range from room to solidus temperatures [6]: it was confirmed in experiment by TEM (Fig. 27) [30]. The hardness of the $Co_{70}Mo_{30}$ alloy with the structure shown in Fig. 27 amounts to 850 HV at room temperature. At a temperature close to the solidus temperature (1335 °C), an ordering–

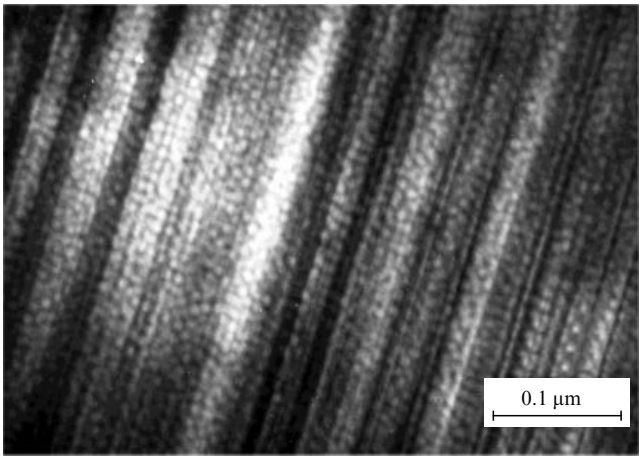

Figure 27. $Co_{70}Mo_{30}$ binary alloy. Quenching from 1300 °C in water. Cellular separation microstructure.

separation phase transition occurs in the $Co_{70}Mo_{30}$ alloy, meaning that chemical compounds can form in this alloy only at temperatures higher than that [30].

Diffusion processes in the $Co_{53}Mo_{35}Cr_{12}$ alloy were regarded in [31] as proceeding in three diffusion couples, viz. Co/Mo, Co/Cr, and Mo/Cr. It was supposed that phase transitions in these diffusion couples are analogous to those in the respective binary alloys of Co–Mo, Co–Cr, and Mo–Cr systems. Clearly, the succession and completeness of these phase transitions depend on the heat treatment temperature and the ratio of chemical affinities of elements in a given diffusion couple at each temperature.

The ratio of Co to Cr atoms in a Co/Cr diffusion couple of the alloy of interest is nearly 4:1. According to the commonly accepted Co–Cr phase diagram of a binary alloy [14], the solid solution A1 begins to separate into layers when its temperature falls to below 900 °C. In accordance with the same diagram, its structure above 900 °C is a solid solution, even if it is actually unknown. It can be supposed that at a higher temperature this alloy also shows a tendency toward separation, because in this system with a composition close the equiatomic one it begins directly from the liquid state [14].

Figure 28 shows fairly large interconnected particles observed after quenching from temperatures in the liquidus-

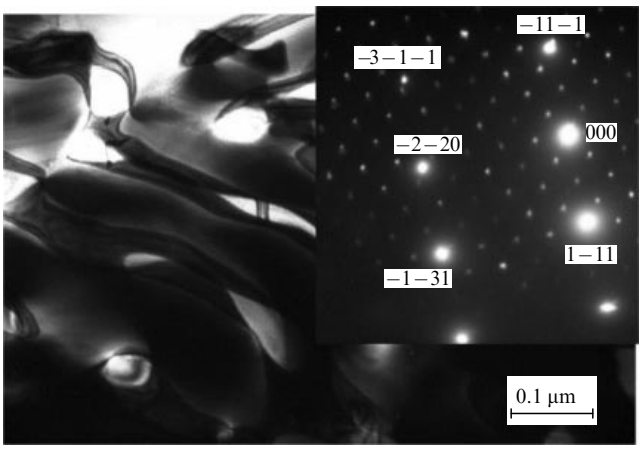

Figure 28. $Co_{53}Mo_{35}Cr_{12}$ alloy. Quenching from the solid state. Inset: electron diffraction pattern obtained from the Co_3Mo phase.

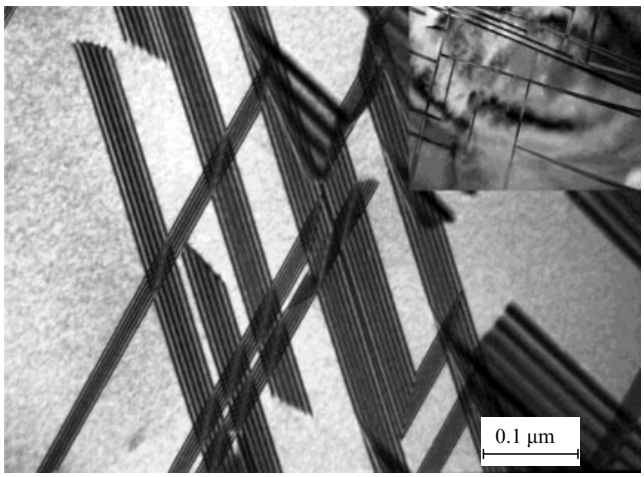

Figure 29. $Co_{53}Mo_{35}Cr_{12}$ alloy. Quenching from the solid state. Inset: stacking faults perpendicular to the foil plane.

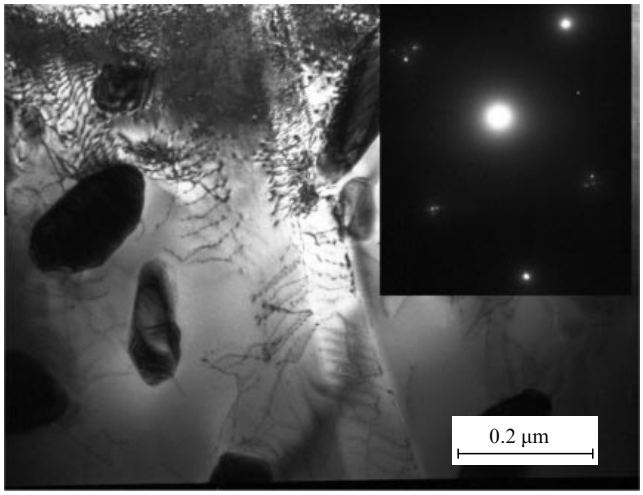

Figure 30. $Co_{53}Mo_{35}Cr_{12}$ alloy. Quenching from 1000 °C. Particles of Cr atoms.

solidus range. Their outer contours suggest that they formed in the absence of elastic resistance of the surrounding medium, i.e., in a liquid solution. The electron diffraction pattern presented in the inset of Fig. 28 gives evidence that such particles have the $D0_{19}$ hexagonal structure inherent in the Co_3Mo phase.

The thermal treatment of the alloy at 1250 °C for 1 h results in complete dissolution of Co_3Mo-phase particles formed in the liquid state of the alloy. A microstructure with a large number of stacking faults is observed (Fig. 29), giving evidence of the low stacking fault energy in this structure. Another region of this foil contains aggregates of BCC-phase particles of chromium atoms formed during separation in Co/Cr and Mo/Cr diffusion couples (Fig. 30).

7.4 Changes in the electronic structure of alloys associated with the ordering–separation phase transition

The discovery of ordering–separation phase transition in many alloys helped in understanding that chemical interactions between component atoms govern all diffusion processes leading to the formation of various phases in these materials. The question is: what is the cause of this

transition? Clearly, changes in the type of microstructure, including the ordering–separation phase transition, are impossible without related changes to the alloy electronic structure. Therefore, Ref. [32] was designed to analyze changes in the electronic structure by comparing them with microstructural changes associated with the ordering–separation phase transition.

Fundamental properties of solids are known to depend on the character of chemical bonds between the nearest neighbors. By chemical bond is usually meant a totality of all forces acting on each atom in a solid and maintaining it in an equilibrium position. Atoms are held together by strong chemical bonds of three main types, viz. metallic, ionic, and covalent. It is currently accepted that metallic bonds arise in metals when valence electrons collectivize to produce electron gas. Collectivization of valence electrons occurs not only in pure metals but also in alloys. However, the presence of two or more kinds of metal atoms involved in a variety of chemical interactions in alloys results in the formation of strong chemical bonds of two other types, ionic and covalent. An ionic bond forms when one or more pairs of valence electrons participating in electron gas production are localized on two neighboring dissimilar atoms and cause the formation of common orbitals. A covalent bond arises when one or more pairs of valence electrons that ought to participate in electron gas production become involved in the formation of hybridized orbitals between similar atoms. Such is, in brief, the modern concept of the nature of chemical bonds in metals and alloys.

Comparing it with the data on microstructures formed in the ordering–separation phase transition as presented in this article gives the feeling that the same phenomenon is considered in both cases, even if described using different terms. Indeed, in an A(B) the ionic component of the bond between B atoms of the dissolved component and solvent A atoms (their nearest neighbors) alloy is manifested when a B atom diffusing in the A(B) lattice finds itself in the immediate proximity to an A atom. This instantaneous neighborhood results in the localization of a pair of valence electrons on these two dissimilar atoms with the formation of common orbitals. At the microstructural level, the alloy displays a tendency toward ordering and the chemical compound A_mB_n forms.

The covalent constituent of the chemical bond manifests itself when two B atoms of the dissolved component diffusing in the alloy happen to become nearest neighbors. As a result, some pairs of their valence electrons become involved in the formation of hybridized orbitals between these two atoms. At the microstructural level, the alloy shows a tendency toward separation and clusters of B atoms are formed.

It is clear that the tendency to ordering develops from the presence of both metallic and ionic components of the chemical bond between A and B atoms, while the tendency toward separation arises due to the existence of the covalent component, besides the metallic one, of the chemical bond between B atom pairs. In other words, the ordering–separation phase transition includes two elementary acts, viz. delocalization of valent electrons on A and B atoms and hybridization of some valence electrons on paired B atoms. In contrast, the separation–ordering phase transition occurs via dehybridization of valence electrons on the pairs of B atoms and localization of some valence electrons on A and B atoms. This transition occurs by virtue of electron-phonon interaction, resulting in the emission of a phonon upon disintegration of a pair of metal atoms connected, for example, by an ionic bond; the subsequent formation of a pair of covalently bound atoms leads to phonon absorption. Such an electron transition implies that a change in the temperature of thermal treatment of an alloy may cause the substitution of the ionic component of the chemical bond between atoms by the covalent one and vice versa.

It follows from the foregoing that the ordering–separation phase transition apparent at the microstructural level as a change in the sign of the energy of chemical interaction between atoms A and B manifests itself in exactly the same way at the electronic level. It is the transition from the state in which all pairs of valence electrons localized on A and B atoms and forming ionic bonds between them leave this state, while pairs of some valence electrons become involved in the formation of hybridized orbitals between two B atoms (which leads to aggregation of B atoms, i.e., separation). This allows such a transition to be referred to as the transition from localization to hybridization of that part of the valence electrons that do not participate in the formation of metallic bonds. The data obtained permit concluding for the first time that the ionic constituent of the chemical bond can transform into the covalent one and vice versa under the proper conditions (a change in temperature and/or alloy composition). Evidently, the cause of the ordering–separation phase transition at the microstructural level is the covalent bond↔ionic bond electron transition [32].

Microstructural changes in alloys associated with this transition occur much later, because the diffusion transition in a microstructure takes a few orders of magnitude longer time than the electronic transition from covalent to ionic bond.

7.5 Diffusion couples in multicomponent alloys

The processes in multicomponent alloys are not as readily understood as in binary ones, largely because it is not clear how diffusion pairs of component atoms are formed in the former materials. Certainly, the introduction of a new component C into an AB alloy does not change the nature of chemical interaction between A and B atoms but only adds new interactions (A–C and B–C). Therefore, the formation of new phases in multicomponent alloys follows the same laws as in the respective binary alloys, even if this process is confined to a microscopic region containing a given diffusion couple. The question is: what are the causes responsible for the formation of microscopic regions whose composition corresponds to one diffusion couple or another in multicomponent alloys? An analysis of all possible chemical interactions in such alloys brought the author of [33] to the conclusion that the causes are exactly the same as in any binary alloy, i.e., covalent and ionic chemical bonding between component atoms.

This makes it understandable why electron microscopy reveals different microstructures in different microregions of a foil of one and the same multicomponent alloy; the alloy was already separated into microscopic sites prior to solidification, which means that none of the freshly smelted ingots actually has the homogeneous solid solution microstructure as it was thought to have before. Rather, it is a structure composed of microscopic regions, each having a chemical composition corresponding to one diffusion couple or another. The size of these microscopic regions remains unaltered after each consecutive thermal treatment, because the temperature of all such treatments is below the solidifica-

tion temperature of the alloy already separated into diffusion couples. At the same time, each following treatment has a different effect on the alloy microstructure in each diffusion pair. A change of the chemical interaction energy sign (the ordering–separation phase transition), concurrent with a change in the treatment temperature, alters the type of microstructure in the corresponding diffusion pair. In the absence of such a transition, a change in the heating temperature affects only the dispersity of pre-existing particles of the same phase.

7.6 Conclusion of the section "Multicomponent alloys"

1. Chemical interactions between dissimilar atoms in all multicomponent alloys are realized based on the principle of pairwise chemical interaction. In ABC multicomponent alloys, this interaction is due to the fact that such alloys are already separated into A/B, A/C, and B/C diffusion couples in the liquid state. The process of such separation proceeds only in the liquid state when the diffusion mobility of the atoms is very high and resistance of the surrounding medium relatively low. Its driving force is constituted by ionic and covalent components of the chemical bond. The separation results in the formation of microregions in the alloy, each containing one diffusion couple or another, in which atoms are held together by either covalent or ionic bonds responsible for the separation or ordering tendency, respectively. Due to this, quenching the alloy in water from the liquid state produces on the same foil different microstructures corresponding to a certain diffusion couple.

2. The ordering–separation phase transition occurs in many diffusion couples of a multicomponent alloy as the temperature of heating changes. It is accompanied by a surprising phenomenon of reversal of the sign of chemical interaction between dissimilar atoms in binary alloys and the respective diffusion couples in multicomponent alloys at a given temperature. The sign reversal is associated with the alteration of the type of microstructure; specifically, the former microstructure dissolves and a new one corresponding to the new chemical interaction energy sign forms. It is therefore very important for the development of new multicomponent alloys to know the ordering–separation phase transition temperature of a binary alloy with the composition corresponding to that of one diffusion couple or another of the future multicomponent alloy.

3. It is proposed to create a structural data bank for each family of multicomponent alloys to store all experimental results, including the ordering–separation phase transition temperature (line) obtained with the use of TEM for binary alloys having a composition similar to that of one diffusion couple or another present at a high concentration in the multicomponent alloy being studied. The availability of such data for a binary alloy would facilitate the prediction of properties and structural changes in the respective diffusion couples of a multicomponent alloy to be produced.

8. Conclusion

1. The view of any physical phenomenon varies with time, usually in accordance with the level of technology available for experimental studies at a given period. An unenviable fate awaits the majority of the proposed theories and hypotheses. Suffice it to mention the once popular classical 'new phase nucleation and growth' theory, the theory of in situ nucleation of special carbides in doped steels, etc. Where are they now? Most of them sank into oblivion in the course of time, because they failed to adequately describe the processes taking place in alloys. However, some of them dating back to the past century have a different fate: they are so deeply rooted in our consciousness that they are still held as the ultimate truth, though they remain unconfirmed in experiment. For example, we can not imagine an equilibrium phase diagram lacking in solid solution regions at high temperatures, although they do not represent an equilibrium phase from the thermodynamic standpoint and therefore must not be put into the diagram. Nor do we imagine the probability of decomposition of a quenched solid solution without its 'supersaturation' with a dopant at low temperature. The same is true of a thermal treatment designed to obtain a highly dispersed structure without preliminary high-temperature quenching from the solid solution region. The observation of ordering–separation phase transitions in alloys may help to rid us of these illusions.

2. Any natural solution consisting of dissimilar atoms is imperfect. Therefore, it tends to decompose at temperatures making component atoms capable of relatively long-range diffusion. This axiom has been accepted in thermodynamics for a long time and refers to all solid solutions in metallic alloys. At the same time, most equilibrium phase diagrams constructed thus far for binary metal systems contain regions of solid solutions, especially at high temperatures, when the diffusion mobility of dissimilar atoms and the energy of chemical interaction between them are sufficient for decomposition. In other words, existing phase diagrams include regions in which the phase (solid solution) is not an equilibrium one.

3. The ordering–separation phase transition that we observed in experiment occurs in the majority of binary alloys. It consists of a change of the sign of the energy of chemical interaction between dissimilar atoms in binary alloys at a heating temperature specific to each system; sometimes, the sign is reversed as alloy concentration changes. This surprising phenomenon is observed at certain temperatures in binary alloys and diffusion pairs of an equivalent composition in multicomponent alloys. As a result, the type of microstructure changes: the former microstructure dissolves and a new one corresponding to the new sign of the chemical interaction energy forms. It is therefore very important for the development of new multicomponent alloys to know the ordering–separation phase transition temperature of a binary alloy with the composition corresponding to that of one diffusion couple or another of the future multicomponent alloy.

4. The discovery of the ordering–separation phase transition in alloys and its explanation in terms of the electron theory of alloys (the ionic bond — covalent bond electron transition) radically changes traditional assumptions in material science. The occurrence of such a transition in nature means that all former views of the solid solution and its decomposition due to a reduction in solubility with decreasing temperature do not correspond to reality. The introduction of the diffusion couple concept completely changes our insight into the new phase nucleation process in multicomponent alloys and promotes understanding why only single- and two-component phases precipitate in them. It also makes it possible to close the problem of explaining why quenching alloys from the 'solid solution region' yields a two-phase structure rather than a homogeneous solid solution structure.

5. The existence of such transitions in nature gives evidence that all former views of alloy decomposition as being due to the reduction of solubility with decreasing temperature are outdated and inconsistent with reality. Consequently, phase diagrams based on such principles do not describe real decomposition processes in alloys. Therefore, the introduction of the concept of ordering–separation phase transition changes the general approach to the construction of phase diagrams. It implies the use of TEM as the main method for the study of micro and crystalline structures. Such a reconstruction of phase diagrams should be started by experimental measurement of the ordering–separation phase transition temperature in each binary system (probably in each group of alloys) and plotting these lines onto the respective diagrams. This work can be expected to take many years, bearing in mind the huge number of binary systems in nature.

References

1. Melton K N, Edington J W *Scr. Metall.* **6** 501 (1972)
2. Knights R, Wilkes P *Acta Metall.* **21** 1503 (1973)
3. Ardell A J, Nicholson R B *J. Phys. Chem. Solids* **27** 1793 (1966)
4. Watts A J, Ralph B *Acta Metall.* **25** 1013 (1977)
5. Ericsson T, Cohen J B *Acta Crystallogr. A* **27** 97 (1971)
6. Higgins, Wilkes P *Phil. Mag. 8* **25** 599 (1972)
7. Ustinovshchikov Yu I, Pushkarev B E *Phys. Usp.* **49** 593 (2006); *Usp. Fiz. Nauk* **176** 611 (2006)
8. Ustinovshikov Y, Pushkarev B, Igumnov I *J. Mater. Sci.* **37** 2031 (2002)
9. Khachaturyan A G *Theory of Structural Transformations in Solids* (New York: Wiley, 1983); Translated from Russian: *Teoriya Fazovykh Prevrashchenii i Struktura Tverdykh Rastvorov* (Moscow: Nauka, 1974)
10. Ustinovshikov Y, Shirobokova M, Pushkarev B *Acta Mater.* **44** 5021 (1996)
11. Ustinovshikov Y, Shabanova I *J. Alloys Comp.* **578** 292 (2013)
12. Ustinovshikov Y, Shabanova I *Mater. Chem. Phys.* **129** 975 (2011)
13. Ustinovshikov Yu I, Shabanova I N, Lomova N V *J. Adv. Microsc. Res.* **8** 27 (2013)
14. Okamoto H, Schlesinger M E, Mueller E M (Eds) *ASM Handbook* Vol. 3 *Alloys Phase Diagrams* (Materials Park, OH: ASM Intern., 1992)
15. Aoki Y, Echigoya J *Scr. Metall.* **19** 639 (1985)
16. Ustinovshikov Y *J. Alloys Comp.* **639** 669 (2015)
17. Ustinovshikov Yu I, Pushkarev B E *Russ. Metall. Metally* **2005** 315 (2005); *Metally* (4) 32 (2005)
18. Ustinovshikov Y *J. Alloys Comp.* **528** 141 (2012)
19. Ustinovshikov Y *J. Alloys Comp.* **575** 10 (2013)
20. Ustinovshikov Y *J. Alloys Comp.* **543** 227 (2012)
21. Ustinovshikov Y *Mater. Chem. Phys.* **165** 14 (2015)
22. Ustinovshikov Y *J. Alloys Comp.* **614** 113 (2014)
23. Ustinovshikov Y *J. Alloys Comp.* **588** 470 (2014)
24. Tiley J et al. *Acta Mater.* **57** 2538 (2009)
25. Jacob K T, Kumar B V *Z. Metall.* **77** 207 (1986)
26. Cieslak M J, Headley T J, Romig A D *Metall. Trans. A* **17** 2035 (1986)
27. Davis J R *Nickel, Cobalt, and Their Alloys* (Materials Park, OH: ASM Intern., 2000) p. 362
28. Day J, Huang X, Yao M *J. Mater. Eng. Perform.* **13** 158 (2004)
29. Nsoesie S et al. *Int. J. Mater. Mech. Eng.* **2** (3) 48 (2013)
30. Ustinovshikov Y, Shabanova I *Mater. Chem. Phys.* **135** 254 (2012)
31. Ustinovshikov Y *J. Alloys Comp.* **602** 135 (2014)
32. Ustinovshikov Y *J. Alloys Comp.* **714** 476 (2017)
33. Ustinovshikov Y *J. Alloys Comp.* **735** 2298 (2018)